



RESEARCH ARTICLE

10.1029/2025MS005035

Key Points:

- Two distinct values of convective available potential energy relaxation timescale, τ , over land and ocean in the convective parameterization scheme are prescribed
- The mean climate stays qualitatively the same, except for a moister and colder near-surface atmosphere for longer τ over the oceans
- A primary gain of using two different τ for land and ocean is improved simulation of the Madden–Julian oscillation propagation features

Supporting Information:

Supporting Information may be found in the online version of this article.

Correspondence to:

B. B. Goswami,
bgoswami@ista.ac.at


Citation:

Goswami, B. B., Polesello, A., & Muller, C. (2025). An assessment of representing land-ocean heterogeneity via CAPE relaxation timescale in the Community Atmospheric Model 6 (CAM6). *Journal of Advances in Modeling Earth Systems*, 17, e2025MS005035. <https://doi.org/10.1029/2025MS005035>

Received 18 FEB 2025

Accepted 22 JUL 2025

An Assessment of Representing Land-Ocean Heterogeneity via CAPE Relaxation Timescale in the Community Atmospheric Model 6 (CAM6)

Bidyut Bikash Goswami¹ , Andrea Polesello¹ , and Caroline Muller¹

¹Institute of Science and Technology Austria (ISTA), Klosterneuburg, Austria

Abstract The time needed by deep convection to bring the atmosphere back to equilibrium is called convective adjustment timescale or simply adjustment timescale, typically denoted by τ . In the Community Atmospheric Model (CAM), τ is the convective available potential energy (CAPE) relaxation timescale and is 1 hr, worldwide. Observational evidence suggests that τ is generally longer than 1 hr. Further, continental and oceanic convection are different in terms of the vigor of updrafts and can have different longevities. So using $\tau = 1$ hour worldwide in CAM has two potential caveats. A longer τ improves the simulation of the mean climate. However, it does not address the land-ocean heterogeneity of atmospheric deep convection. We investigate the prescription of two different CAPE relaxation timescales for land ($\tau_L = 1$ hr) and ocean ($\tau_O = 1$ to 4 hr). It is arguably an extremely crude parameterization of boundary layer control on atmospheric convection. We contrast a suite of 5-year-long simulations with two different τ for land and ocean to having one τ globally. The choice of longer τ over ocean is guided by previous studies and inspired by observational pieces of evidence. Nonetheless, to complement our variable τ_O experiments, we perform a simulation with $\tau_O = 1$ hr and $\tau_L = 4$ hrs. Most importantly, our key findings are immune to the exact values of prescribed τ_L and τ_O . The CAM model, with two τ values ($\tau_O > \tau_L$), improves convective-stratiform rainfall partitioning and the Madden–Julian oscillation propagation characteristics.

Plain Language Summary A thermodynamically unstable atmosphere releases its energy by creating clouds. Deep clouds take time to decay and bring the atmosphere back to equilibrium. The decay time of deep clouds is called convective adjustment timescale or simply adjustment timescale, typically denoted by τ in climate model formulations. In the Community Atmospheric Model it is defined as the convective available potential energy consumption time scale and set to 1 hr globally. Since convection behaves differently over land and sea using different values of τ for continents and oceans could better represent their distinct convection behaviors. Our climate simulations using CAM showed that setting τ over the oceans to 4 hr and τ over continents to 1 hr improved the accuracy of the simulations, particularly for the Madden-Julian Oscillation. It suggests that using two different τ values for continent and ocean is recommended.

1. Introduction

Deep convection is complex to parameterize (Arakawa, 2004). While the explicit representation of deep convection is becoming a plausible option to navigate this “deadlock” (Randall et al., 2003; Randall, 2013), for long-term projections of our climate, cumulus parameterization is still unavoidable. Hence, amidst a rapid emergence of convection-resolving models (Stevens et al., 2019), various schemes to parameterize convection continue to develop. In particular, the recent decades have witnessed a surge of novel ideas that have accelerated this progress (Rio et al., 2019, and references therein).

The “art” of tuning parameters used in convection parameterization schemes, or simply parameter tuning, plays a vital role in this development process (Hourdin et al., 2017). While deficiencies of convective parameterization are primary factors for model biases, it alone cannot alleviate all model biases (Goswami et al., 2017). Hence, parameter sensitivity investigations are necessary not only to optimize the performance of a scheme but also to understand the extremities to which a scheme can be held responsible for biases in a simulation (Qian et al., 2015; Goswami et al., 2017). In this study, we aim to contribute to understanding one tunable parameter, the CAPE relaxation timescale τ , by investigating the sensitivity of climate simulations to two different τ values for land and ocean in contrast to having one value globally in the Zhang-McFarlane (ZM) convective parameterization scheme

(Zhang & McFarlane, 1995, ZM95 hereafter) in the Community Atmospheric Model (CAM), the atmospheric model of the Community Earth System Model (Danabasoglu et al., 2020).

In CAM, deep convection is represented using the ZM convection parameterization scheme. The ZM is an adjustment-type convective parameterization scheme where the atmospheric instability is removed via an adjustment toward a background level of convective stability. In ZM, convective available potential energy (CAPE) defines atmospheric instability, and τ is the CAPE relaxation timescale. The CAPE relaxation timescale τ , also known as the convection consumption time, or the convection relaxation time is not exclusive to the ZM scheme. Since introduced by Fritsch and Chappell in the early 80 s (Fritsch & Chappell, 1980), τ was used in the Kain–Fritsch scheme (Kain & Fritsch, 1993) and in several other schemes in addition to in ZM, for example, the Betts–Miller–Janjic (BMJ) scheme (Betts & Miller, 1986, 1993) (uses τ as the timescale of a parcel's thermodynamic profile to adjust toward a reference background profile), the relaxed Arakawa–Schubert scheme (Moorthi & Suarez, 1992), Grell–Freitas convection scheme (Grell & Freitas, 2014) (uses an effective measure of τ that depends on model grid resolution and a base convective adjustment timescale of 1–3 hr), Bechtold et al. (2001, 2008), etc.

To quote ZM95, “The adjustment time scale determines the intensity and duration of convection for a given CAPE. With small τ the convection is short-lived but intensity is high, on the other hand, with larger τ the convection is long-lived but of low intensity.” ZM95 used τ values of 2, 4, and 6 hr and reported their scheme to be particularly sensitive to the choice of τ (also see, Scinocca & McFarlane, 2004; Yang et al., 2013). Since there is no strict range of τ , several studies investigated the sensitivity of CAM simulations to different τ values. For example, Mishra and Srinivasan (2010) used $\tau = (1, \infty)$. Contrasting water–vapor–isotope simulations in a suite of CAM single-column simulations with a range of τ values, Lee et al. (2009) found their simulations to match better with satellite observations with $\tau = 8$ hr. Mishra (2011, 2012) prescribed $\tau = 8$ hr in global climate simulations and noted improvements in the simulations of tropical climate, especially the convectively coupled equatorial waves (CCEWs). In all of the above studies, τ has a single value globally.

One value, 1 hr, of τ globally in CAM has two potential caveats. One, observations suggest a longer adjustment time scale. Analyzing the moisture-to-rainfall conversion efficiency of the atmosphere, Bretherton et al. (2004) estimated the convective moisture adjustment time scale (τ_{moist}) and suggested that it should be approximately 12 hr. Focusing on the Indo-Pacific warm pool region, Shin and Baik (2023) found τ_{moist} to be 17 hr, and Mayta and Adames Corraliza (2023) suggested τ_{moist} should be about 1 day. Studies that focus on τ_{moist} report its values ranging from a few hours to about a day. It is noteworthy that, τ_{moist} is the time scale in which moisture anomalies are adjusted in the atmosphere through convective processes. Therefore, unlike τ , it only considers adjustment of moisture, not temperature (Ahmed et al., 2020). Considering temperature contributions, Ahmed et al. (2020) argued a τ value of ~ 2 hr is realistic. In one of the earliest attempts of adjustment-type convection parameterization frameworks, Betts (1986) used a τ value of 1–2 hr. Current GCMs continue to use τ values ranging from an hour to a few hours that are obtained by assessing model sensitivity (Bullock et al., 2015; Wang et al., 2024). A trial-and-error approach of finding a “sweet-spot” τ value is guided by the extreme sensitivity of model performance on the value of τ [e.g., Emanuel et al., 1994; Alapaty, Raman, et al., 1994; Alapaty, Madala, & Raman, 1994; Lin et al., 2000]. In particular for the CAM model that uses the ZM-scheme, evaluating 22 tunable parameters Qian et al. (2015) reported τ as one of the most critical tuning parameters. It is still poorly understood yet remains an attractive tuning parameter for improving GCM performance and longer values were argued to improve model performance, for example, 8 hr in Lee et al. (2009) and Mishra (2011, 2012). Using the National Oceanic and Atmospheric Administration's Geophysical Fluid Dynamics Laboratory atmosphere model, Zhao et al. (2018) also used a relaxation time of 8 hr in a cloud work function relaxation closure for convection parameterization. A choice of long τ values, ~ 8 hr, in various model tuning studies leaves “ $\tau = 1$ hr” demanding more investigation. Caveat number two is, one value of τ globally is not a logical choice because deep convection exhibits different behaviors over continents and oceans (Hagos et al., 2013; Matsui et al., 2016; Roca et al., 2017; Roca & Fiolleau, 2020). Since the width of a thermal plume is steered by boundary layer height (Williams & Stanfill, 2002), a deep continental boundary layer generates wider updraft velocities in deep convection (Lucas et al., 1994). Matsui et al. (2016) provided a climatological view of the contrast between oceanic and continental convective precipitating clouds from long-term Tropical Rainfall Measurement Mission (TRMM) satellite multisensor statistics. They found large proportions of deep clouds over land. Zipser et al. (2006) also found the most intense storms typically over continents. Intense storms require stronger updrafts which lead to faster restabilization response (hence a shorter τ) for the atmosphere to adjust. These observations suggest that the

atmospheric deep convection over land is wider and stronger than those over the oceans. In other words, atmospheric convection over land is shorter lived than that over ocean (Roca et al., 2017). Analyzing the relationship between precipitation and column relative humidity over continents and oceans, Ahmed and Schumacher (2017) found a lower critical column relative humidity threshold over land at which precipitation intensifies significantly. A smaller humidity threshold implies that convection responds by producing precipitation at lower humidity levels over land than over the oceans. It suggests that the atmosphere adjusts more quickly to moisture changes, which indicates a faster adjustment time scale over land than over the oceans. Ahmed and Schumacher (2017) further reported a detailed geographical variation in humidity threshold for producing precipitation. As a first attempt, considering the aforementioned observational suggestive evidence, we prescribe a shorter CAPE consumption time scale over land than over oceans. Furthermore, logically, as a zero-order argument, convection of equal strength can be posited to decay faster over land compared to over oceans due to limited moisture supply to sustain convection, and rapid cooling of the land surface (reducing thermal forcing) soon after initiation of precipitation. It motivated us to address the following question: although two different τ values incorporating land-ocean inhomogeneity are logical, is it fruit-bearing in a model-simulated climate? To answer this question, we investigate, the response of the mean climate and of large-scale waves, by contrasting 5-year-long climate simulations with and without incorporating land-ocean inhomogeneity via τ values. Our approach of using two τ values for land and ocean arguably is a crude way to parameterize the effect of heterogeneity in the drivers of convection over land and ocean and is unable to capture the detailed physics of it, for example, of boundary layer processes as a control on convection (Donner & Phillips, 2003). Analyzing the impacts of boundary layer processes on CAPE, Donner and Phillips [2003] reported larger CAPE values over land and estimated longer τ over land than over oceans. Their analysis was based on data collected over midcontinent North America, the tropical east Atlantic, and the tropical west Pacific. The longer τ over land apparent in Donner and Phillips (2003) indicates a finer geographical variation τ which is beyond our crude prescription of two τ values.

Convective parameterization schemes, particularly adjustment-type schemes, are based on the idea that convection takes some time to stabilize the atmosphere to a background state. Essentially, this time taken is τ in the ZM scheme. Although numerically τ can have almost any value, it is decided based on a scale separation between the convective activity of the individual clouds and large-scale forcing. This concept is nicely depicted in Figure 1.1 of (Davies, 2008). The graph in that figure is a function of timescales associated with convection, and consists of a turbulent initial segment indicating fluctuation of individual clouds, followed by a flat segment where these fluctuations smooth out, and finally a segment corresponding to longer time-scales that shows the evolution of the large scale forcing field itself. Conceptually, changing τ within a reasonable range (within the flat segment of Figure 1.1 of (Davies, 2008)) should not result in a dramatic change in the mean state of the simulated climate. Nonetheless, we expect to see some model responses in simulations of convective and large-scale precipitation (Scinocca & McFarlane, 2004). We shall investigate it in detail in the first part of our results section.

Some changes that we expect in our experiments are in the simulated organization of convection. The organization of convection comes from the dynamic and thermodynamic impacts of convection on the atmosphere. Simply put, it is the memory of convection (Davies et al., 2009), that is the fact that convection changes the large-scale properties, and can make their environment favorable or unfavorable to subsequent convection. Identifying sources of convective memory in cloud-resolving simulations, Colin et al. (2019) argued that the persistence of the state of convection contributes to convective memory. Colin et al. (2019) also suggested that convective memory and organization interact mutually. By altering τ we essentially alter memory associated with convection. Hence, we expect to see changes in convective organization. Taking a cue from Mishra (2011), we anticipate improved convective organization in the tropics for longer τ . However, land-ocean heterogeneity in τ is a unique feature of our experiments that we argue is essential based on heterogeneity in the behavior of convection over land and ocean. As supporting evidence, we shall present an analysis of equatorial waves focusing on the MJO to evaluate the organization of convection in the second part of our results section. Although our analyses are based on 5 years long model simulations which is not an ideal length of a simulation to analyze MJO activity, it is nonetheless long enough to assess a model's overall behavior and fidelity in simulating MJO or similar intra-seasonal variability (e.g., Zhang & Song, 2009; Goswami et al., 2015).

This paper is organized as follows. A brief description of the methodology is provided in Section 2, including model experiment design and details of the experimental τ values used in the experiments. A brief assessment of the model acceptability of the experimental τ values is provided in Section 3.1 and the model response in terms of

Table 1
 τ Values for Different Experiments

Experiment name	τ_L	τ_O
$EXPT_{fast}$	1 hr	1 hr
$EXPT_{2h}$	1 hr	2 hr
$EXPT_{3h}$	1 hr	3 hr
$EXPT_{4h}$	1 hr	4 hr
$EXPT_{slow}$	4 hr	4 hr

mean climate is documented in Section 3.2. Emphasizing the key model responses, a convective-stratiform rainfall partitioning analysis is provided in Section 3.3, and MJO simulation analyses are documented in 3.4. Discussion of the results and concluding remarks are provided in Section 4. A key future recommendation and some obvious limitations of this study are provided under subsection 4.4.

2. Model and Simulation Details

We used the atmospheric model of the Community Earth System Model, version 2.1.3 (CESM 2.1.3) (Danabasoglu et al., 2020), that is the CAM, version 6 (Community Atmospheric Model 6 (CAM6)), developed and maintained at the National Center for Atmospheric Research, with longitude and latitude specifications 1.25° and 0.9°, respectively, and 32 vertical levels. We forced the model by HadISST1 climatological monthly mean SST data provided by the Met Office Hadley Centre (Rayner, 2003). In short, we performed CESM “F2000climo” simulations. In general, these are atmospheric simulations forced by present-day climatology. All simulations are 6 years long, and we analyzed the last 5 years of each simulation since, for atmosphere-only simulations, 1-year spin-up is enough.

We performed 5 simulations. The one with out-of-the-box τ value of 1 hr globally is denoted by $EXPT_{fast}$. In the next 3 simulations, we delayed the τ value over ocean (τ_O) to 2, 3, and 4 hr keeping τ over land (τ_L) 1 hr. We called these 3 simulations $EXPT_{2h}$, $EXPT_{3h}$ and $EXPT_{4h}$, respectively. We performed a last 5th experiment, named $EXPT_{slow}$, for which we used a τ value of 4 hr globally. It is important to emphasize that our goal is not to tune the model per se but to investigate whether representing land-ocean heterogeneity via τ improves the CAM model simulation. Therefore, the key is the land-ocean heterogeneity represented by a (τ_L, τ_O) pair rather than their values. Thus, the best pair of τ values may not be the ones that we have prescribed in our experiments. Table 1 depicts the τ values for different experiments. In addition, we also performed an additional simulation with $\tau_O = 1$ hr and $\tau_L = 4$ hrs. We call this simulation $EXPT_{4hLand}$ and, τ value wise, it is inverse of $EXPT_{4h}$. It is essentially a complementary simulation, thus the results from this simulation are presented only in the supplementary document.

Our analyses primarily show a comparison between the 5 simulations mentioned in Table 1. For observation data, we have used TRMM Multi-Satellite Precipitation Analysis (TMPA) 3B42 Version 7 and 3A25 product (Huffman et al., 2007; TRMM Readme, 2017), reanalysis data from 5th generation ECMWF reanalysis product (ERA5) (Hersbach et al., 2023), outgoing long-wave radiation (OLR) from the National Oceanic and Atmospheric Administration (2.5° × 2.5°; daily from 01-June-1974 to 12-December-2019) (Liebmann & Smith, 1996). A cautionary note for the rainfall partitioning analyses presented in Section 3.3 is that convective rainfall definitions in TRMM and climate models are not the same (Dai, 2006; Pendergrass & Hartmann, 2014). As an observational benchmark for Figure S13 in Supporting Information S1, the National Centres for Environmental Predictions reanalysis-I zonal winds are used (1979–2019) (Kalnay et al., 1996).

3. Results

3.1. Model Basic State

We used CAM6 for our modeling experiments. The CAM is a widely used model and its latest version, CAM6, has been tested based on various metrics and is a credible model (Bogenschutz et al., 2018). It has been evaluated for various aspects of the climate, for example, evaluation of basic features like cloud and precipitation (Zhou et al., 2021), chronic issues like the double-ITCZ bias (Woelfle et al., 2019), complex systems like the Indian monsoon (Kumar et al., 2023), etc. For brevity, we refrain from discussing analyses of the model's basic state. Nonetheless, we provide the top of the atmosphere (TOA) radiation budget plots of the $EXPT_{2h}$, $EXPT_{3h}$, $EXPT_{4h}$ and $EXPT_{slow}$ with respect to the out-of-the-box CAM6 version (i.e., our $EXPT_{fast}$ simulation) in Figure S1 in Supporting Information S1. We know from earlier experiments with CAM (Scinocca & McFarlane, 2004; Mishra & Srinivasan, 2010) and theoretical understanding (Davies, 2008), that CAM can accommodate any value of τ . As expected, there was no model failure due to the prescription of our experimental τ values. The TOA energy balance did not exhibit any dramatic or large changes. Precipitation field, in terms of its global mean values also remains roughly unchanged (Figures 1 and 3a–3c, and 4a–4c) albeit it does show some changes in

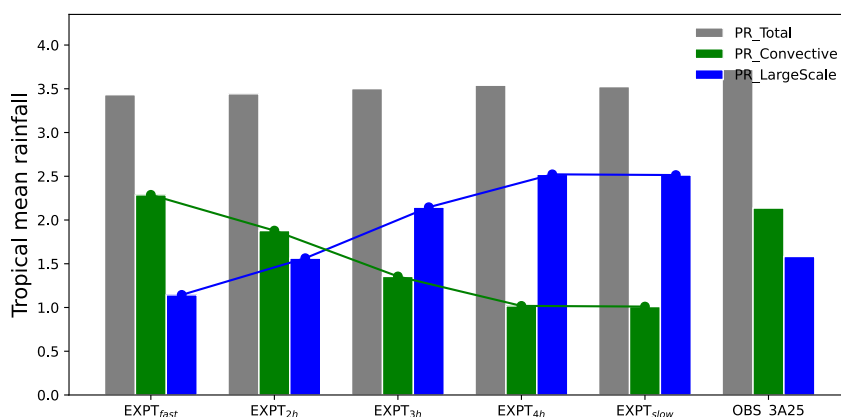


Figure 1. Tropical (tropics defined as the zonal belt between 30°S–30°N) annual mean daily rainfall (mm/day) for different experiments mentioned in Table 1 and Tropical Rainfall Measurement Mission 3A25. The green and blue lines connecting the respective color bars are included for visual guidance.

terms of its spatial distribution (Figure S2 in Supporting Information S1). With these basic state checks of the experimental simulations exhibiting no dramatic model responses, we present our analyses of the model responses in simulating the mean climate and the variability (the equatorial waves) in the following sections.

3.2. Mean Climate

Since about 75% of the global surface is ocean, in the simulations of the mean climate, we expect a similar model response in our experiments by delaying τ only over the oceans, as earlier studies did by having a larger τ globally. An evaluation of some of the mean features of simulated climate in our experiments confirm this. We find an increase in large-scale rainfall and a decrease in convective rain going from *EXPT_{fast}* to *EXPT_{slow}* (Figure 1 and Figure S2 in Supporting Information S1). Similarly, we also notice warming in the lower levels, stronger warming in the upper levels, slight cooling in the mid-levels; moistening in the lower levels, and drying in the mid-levels (Figure 2 and Figure S3 in Supporting Information S1). These features have been reported in earlier studies [for example, Figure 8 in Mishra & Srinivasan, 2010].

The simulated temperature and specific humidity profiles in our simulations are less biased over ocean than over land, when compared with ERA5 data (averaged over the period 2014–2023) (Figure 2a). A significant cold bias is seen over land especially in the lower levels. We found it is partially related to the model interpolation of temperature at pressure levels below the surface level on elevated lands. Indeed, computing these temperature profiles excluding grid points with surface altitude above 1000 m reduces the bias (figure not shown). Investigating model response relative to the *EXPT_{fast}* simulation, we notice in addition lower level (upper level) warming (cooling) is more (less) over land than over oceans (Figure 2b). In the case of moisture, the letter “S” patterned vertical structure over the ocean is more curvy and squeezed down meaning lower level (middle level) moistening (drying) is stronger over oceans than over land and the respective peaks are vertically closer to the sea surface. These profiles, all together, indicate a model response to changes in τ in terms of the distribution of atmospheric convection and clouds, which impacts heating/cooling and moistening/drying of the air column (Figure S3 in Supporting Information S1). Essentially these responses indicate an accumulation of convective instability in the atmosphere with delaying of CAPE relaxation time scale. It is attributable to more low-level warming over the continents and more low-level moistening over the oceans. More moistening near the ocean surface is relatively straightforwardly understandable, and it is a consequence of the atmosphere taking longer to convect with larger τ . To a zero-order approximation, as a result of the near-surface moisture pile-up in the oceanic regions, there is a moisture deficit in the lower levels over the continental regions (Figures S4a–S4c in Supporting Information S1). Indeed we note profound land drying for longer τ (Figure S4a in Supporting Information S1). The consequences are reflected in terms of changes in cloud cover. In an overall declining tendency of cloud cover, from *EXPT_{2h}* to *EXPT_{slow}*, over the tropics high clouds decrease more steeply than low clouds. Low clouds decrease less rapidly over the ocean compared to those over land (Figure S5 in Supporting Information S1). It should be noted that cloud categories are objectively defined in CESM. For example, low-level clouds are the ones below 700 hPa and high clouds are between 400 and 50 hPa. Cloud covers are

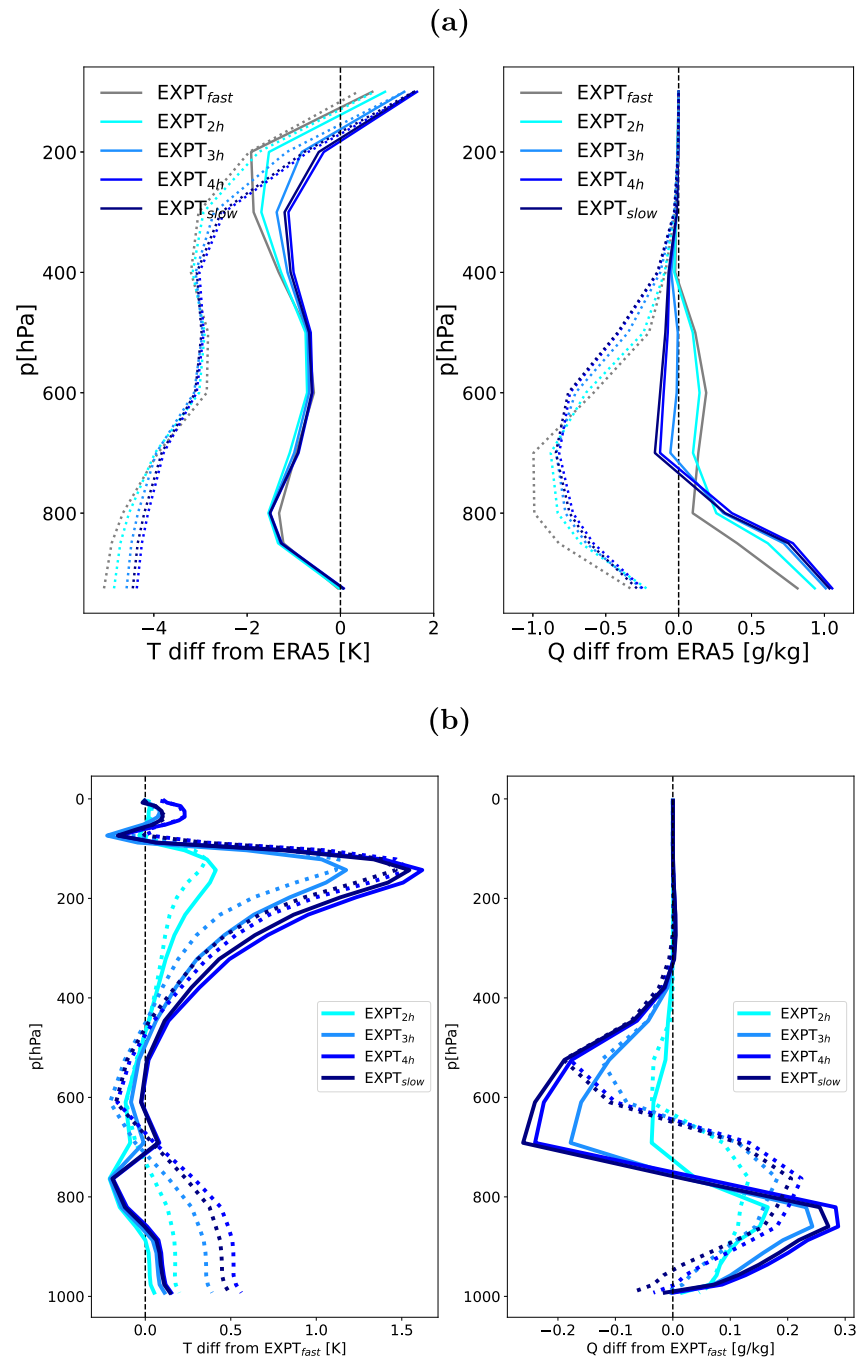


Figure 2. Tropical (tropics defined as the zonal belt between 30°S–30°N) mean vertical profiles of temperature (T) and specific humidity (Q). Departures of different experiments, as indicated in the legends, (a) from ECMWF reanalysis product (2014–2023), (b) from $EXPT_{fast}$ (Land: Dotted, Ocean: Solid). The vertical dashed line indicates the zero departure.

integrated for each model level corresponding to respective cloud categories. In that regard, going from $EXPT_{2h}$ to $EXPT_{slow}$, low-cloud cover changes are consistent with relative surface moistness over land and ocean (comparing Figures S4a and S5a in Supporting Information S1). It is noteworthy here that there is a general tendency of a moister atmosphere in $EXPT_{2h}$ compared to $EXPT_{fast}$, while going from $EXPT_{2h}$ to $EXPT_{slow}$ models exhibit gradual drying. We do not have a clear understanding of this response. Mishra (2012) reported changes in evaporation in their modeling experiments with τ resulting from complex interactions between

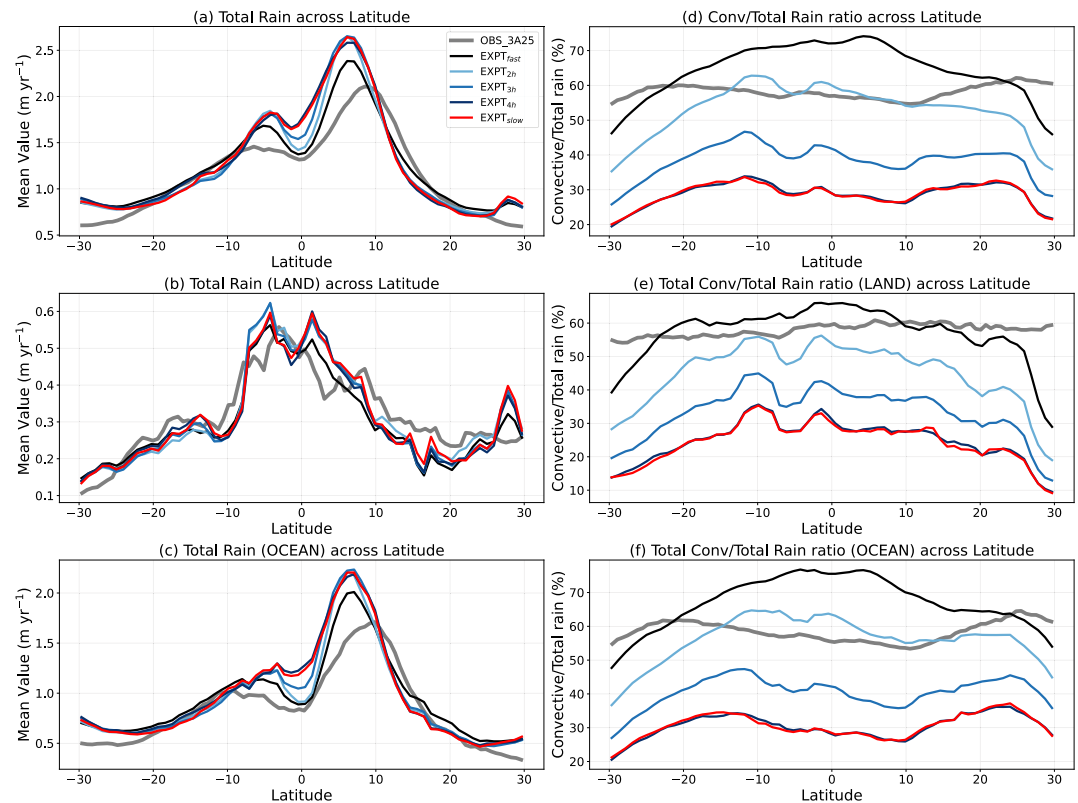


Figure 3. Left hand panels: Zonal mean rainfall over Tropics (from 30°S to 30°N), (a) over the whole tropical belt, (b) over tropical Land, and (c) over tropical Ocean. Right hand panels: Zonal mean Convective-to-Total rainfall ratio (%), (d) over the whole tropical belt, (e) over tropical Land, and (f) over tropical Ocean.

circulation and surface fluxes. Since, in a global mean sense, the humidity changes are rather small in our experiments, this issue will require detailed spatial analysis.

Taken together, the altered vertical profiles of moisture and temperature, distribution of convective and large-scale rainfall, and associated clouds are consistent with the idea that convection is short-lived and stronger for smaller τ values and long-lived and weaker for longer τ value. It is also evident from the solution of the CAPE equation in the ZM scheme, which can be expressed as $CAPE(t) = CAPE_o \exp\left(\frac{-t}{\tau}\right)$ in the absence of large-scale CAPE generation, where $CAPE_o$ is the values of CAPE at $t = 0$. A larger τ in this expression means a slower decay of CAPE. The duration of convection is essentially linked with its persistence and hence “memory.” We discuss its impact on the simulation of the equatorial waves in Section 3.4.

3.3. Convective Versus Stratiform Precipitation

Climate models often tend to overproduce drizzling rain (Chen et al., 2021; Dai, 2006). Models produce light rain events too frequently because of their limitation to mimic processes which allows instability to build up before triggering convection and produce rain. Over the tropics, where intense deep atmospheric convections are abundant, models perform worse (Sun et al., 2006; Dai, 2006; Goswami et al., 2014). In addition, because most intense storms typically occur over continents (Zipser et al., 2006), drizzle bias can be expected to be more prominent over land (Sun et al., 2006). This biased model behavior is a manifestation of unrealistic partitioning of the total rainfall in convective and stratiform type precipitation (Chen et al., 2021). This means the total rainfall might still look realistic, however with a wrong partitioning of convective and stratiform rainfall (Kyselý et al., 2016). Therefore we analyzed the partitioning of rainfall in our experiments computing the contribution of convective rainfall to the total rainfall ($C_{\%}$).

Figures 3 and 4 depict the zonal and meridional mean profiles, respectively, of total rainfall and $C_{\%}$ for the whole tropics and also for land and ocean separately. In these figures, we additionally plotted $C_{\%}$ for TRMM_{3A25}. It

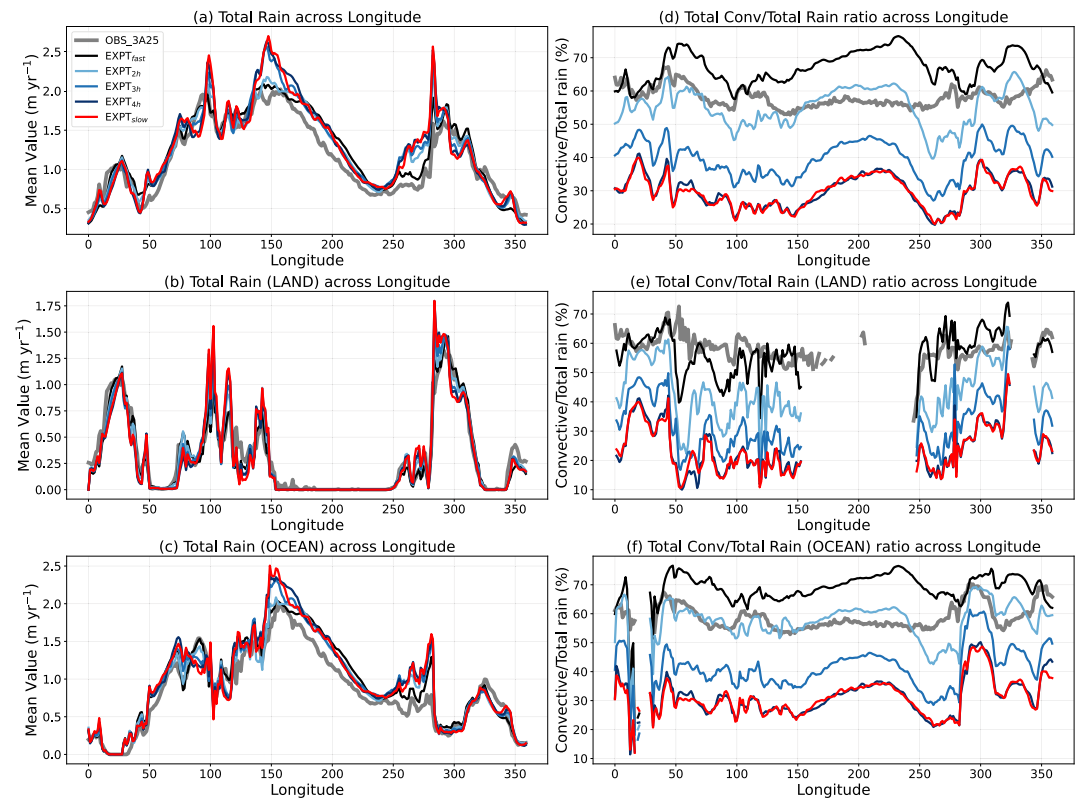


Figure 4. Left hand panels: Meridional mean rainfall over Tropics (averaged over 30°S–30°N), (a) over the whole tropical belt, (b) over tropical Land, and (c) over tropical Ocean. Right hand panels: Meridional mean Convective-to-Total rainfall ratio (%), (d) over the whole tropical belt, (e) over tropical Land, and (f) over tropical Ocean.

should be noted here that, the definition of convective rain is not the same in TRMM_{3A25} and in CAM6, and $C_{\%}$ for TRMM_{3A25} should be seen only as a guidance and not a true comparison. Assessing the zonal and meridional mean plots of total rainfall considering land and ocean together or separately (panels a–c in both the figures), we note, in general, that there are no remarkable differences between the different simulations. $EXPT_{fast}$ is closest to observations, most obvious in the zonal mean of total rainfall over the whole tropics (Figure 3a). However, the right-hand side panels of Figures 3 and 4 show that it is $EXPT_{2h}$, considering the amplitude of the curve, that looks the most realistic of all simulations, especially over the oceans (Figure 3f). In Figures 3 and 4, $EXPT_{fast}$ overestimates convective precipitation while $EXPT_{3h}$, $EXPT_{4h}$, and $EXPT_{slow}$ underestimate it. The pattern of the $C_{\%}$ curves in $EXPT_{4h}$ and $EXPT_{slow}$ most closely resemble observations although the amplitude is weaker. When we consider precipitation values within 10°S–10°N, the bias in $EXPT_{fast}$ are more prominent (Figure S6 in Supporting Information S1).

To summarize the evaluations of the mean state of the simulated climate, $EXPT_{2h}$ is the best version of the model and $EXPT_{fast}$ is the second-best unless we consider a critical detail, namely, the shape of the meridional profile of rainfall partitioning in Figure 3f. Next, we will evaluate the models based on an assessment of the simulation of MJO features.

3.4. Simulation of MJO Variance and Propagation

Organization is a primary feature of tropical convection. It essentially means a cluster of deep precipitating clouds tied together. An important question is, what brings these clouds together? In other words, what causes convection to organize? One idea to see the organization of convection is through superpositions of CCEWs. These atmospheric waves and tropical convection are entangled. In the tropics, the atmosphere responds to convective heating in terms of waves that, in turn, organize convection. Therefore, the fidelity of a model in simulating tropical climate is essentially its ability to simulate the CCEWs. A standard metric to analyze CCEWs is the

Takayabu-Wheeler-Kiladis (TWK) spectra (Takayabu, 1994a, 1994b; Wheeler & Kiladis, 1999). Figure 5 depicts the symmetric and asymmetric TWK-spectra for the observed and simulated OLR. Understandably, a striking feature of the TWK-spectra of observed OLR shown in Figures 5a and 5b is the spectral power near the origin of the plots in the wavenumber range 1–5 and frequency 20–100 days, well known as the MJO. The MJO is a combination of or envelope of other waves in the equatorial atmosphere. Hence, the accuracy of MJO simulation is arguably a measure of the fidelity of accurate simulation of waves in the atmosphere (Zhang et al., 2020). Guo et al. (2015) showed in detail that the accuracy of CCEW simulation is critical for a realistic MJO simulation.

A comprehensive review of the science of MJO is available in Zhang et al. (2020). Prominent observed features of MJO suggest that they are most active in the Indo-Pacific warm pool with an eastward propagation. An interesting fact, along its path from the Indian to the Pacific Ocean, is that an MJO passes over the Indonesian maritime continent (IMC). During this passage, MJO and the prominent diurnal variabilities in the meteorology over the IMC islands interact and mutually influence each other. So much so that nearly half of the MJOs fail to propagate into the Pacific. It is critical, therefore, to represent the land-ocean heterogeneity as realistically as possible in climate models. Hence, we expect our experiments with logically defined different values of τ for land and ocean to improve simulated MJO features. Here, we shall present analyses evaluating the simulation of MJO variance and propagation. We can draw some idea of MJO simulation in different experiments from Figure 5. In Figure 5, the foremost remarkable feature is the increase in spectral power in the MJO wave number and frequency range for experiments with a longer τ . A closer visual inspection reveals that the MJO power in the symmetric spectra does not dramatically change from $EXPT_{2h}$ to $EXPT_{slow}$. In the antisymmetric spectra, the MJO power peaks at wavenumber 2 in $EXPT_{2h}$ but exhibits a standing mode feature (with power at wavenumber 0) in the simulations with longer τ . For other waves, no one simulation is remarkably better than the rest. Figure 5 loosely suggests that overall the symmetric signal waves are improved for longer time scales, but there are no clear improvement for the antisymmetric part.

To bring out the active region of MJO we applied space-time filtering on OLR data containing the signal corresponding to wavenumbers 1–5 and a period of 20–100 days. In Figure 6 the variance of the MJO-filtered daily OLR anomalies is shown. In observations (Figure 6a), the peak variance is over the Indo-Pacific warm pool. Feeble variance peaks are noted in the eastern sides of the Pacific (off the Gulf of California) and Atlantic (around the western coast of Sierra Leone). It is consistent with the fact that although MJO is most active in the Indo-Pacific warm pool region, it has considerable influence modulating the convective activity over the eastern equatorial Pacific (Maloney & Hartmann, 2000a,b; Maloney & Kiehl, 2002) and Atlantic (Klotzbach, 2014). For $EXPT_{fast}$ high variance is noted around the warm-pool region but widely spread and has multiple peaks. The strongest variance is around Northern Australia and the south-western Pacific region. The other secondary maxima are over the southern Bay of Bengal, the central equatorial Indian Ocean, and the central Pacific regions.

The simulated MJO variance strength and pattern experience some changes with changes in τ values. In general, a slower τ_O keeping τ_L same yields more variance over the warm pool region in a relative sense (Figure S11 in Supporting Information S1). In other words, it increases convective activity in MJO space and time scales. The variance fields normalized by the respective domain means are available in Figure S11 in Supporting Information S1, which depicts a better visual illustration of the variance peaks. In $EXPT_{2h}$ a pronounced peak is located over the western-central equatorial Pacific with two secondary maxima near the south-western equatorial Pacific and eastern equatorial Indian Ocean. In $EXPT_{3h}$ the variance is more concentrated over the western equatorial Pacific, with a secondary peak south of the central equatorial Indian Ocean. With larger values of τ_L , the maximum variance gets more and more focused over the warm pool region, from $EXPT_{fast}$ to $EXPT_{3h}$ (comparing Figures 6b–6d). It is noteworthy, that all the pronounced peaks for $EXPT_{2h}$ and $EXPT_{3h}$ are over oceans, in and around the Indo-Pacific warm pool region, but split unlike observations (Figure 6a). The model simulated MJO variance further slowing τ_O to 4 hr ($EXPT_{4h}$ shown in Figure 6e) suggests that MJO variance does not necessarily increase with increasing τ_O . The variance peak intensities are visibly weaker in $EXPT_{04}$ compared to that in $EXPT_{2h}$ and $EXPT_{3h}$ and more only than that in $EXPT_{fast}$. However, a noteworthy feature of $EXPT_{4h}$, a fine detail missing in all other simulations, is that the variance shows a secondary peak near the eastern side of the equatorial Pacific and Atlantic oceans. Baring these subtle variance peaks, $EXPT_{slow}$ looks the best, although still a considerably weaker variance peak compared to observations.

A prominent feature of MJOs is eastward propagation. The propagation features of the MJO are arguably better characterized by Hovmöller plots averaged over the latitude band between 10°S and 10°N, shown in Figure 7.

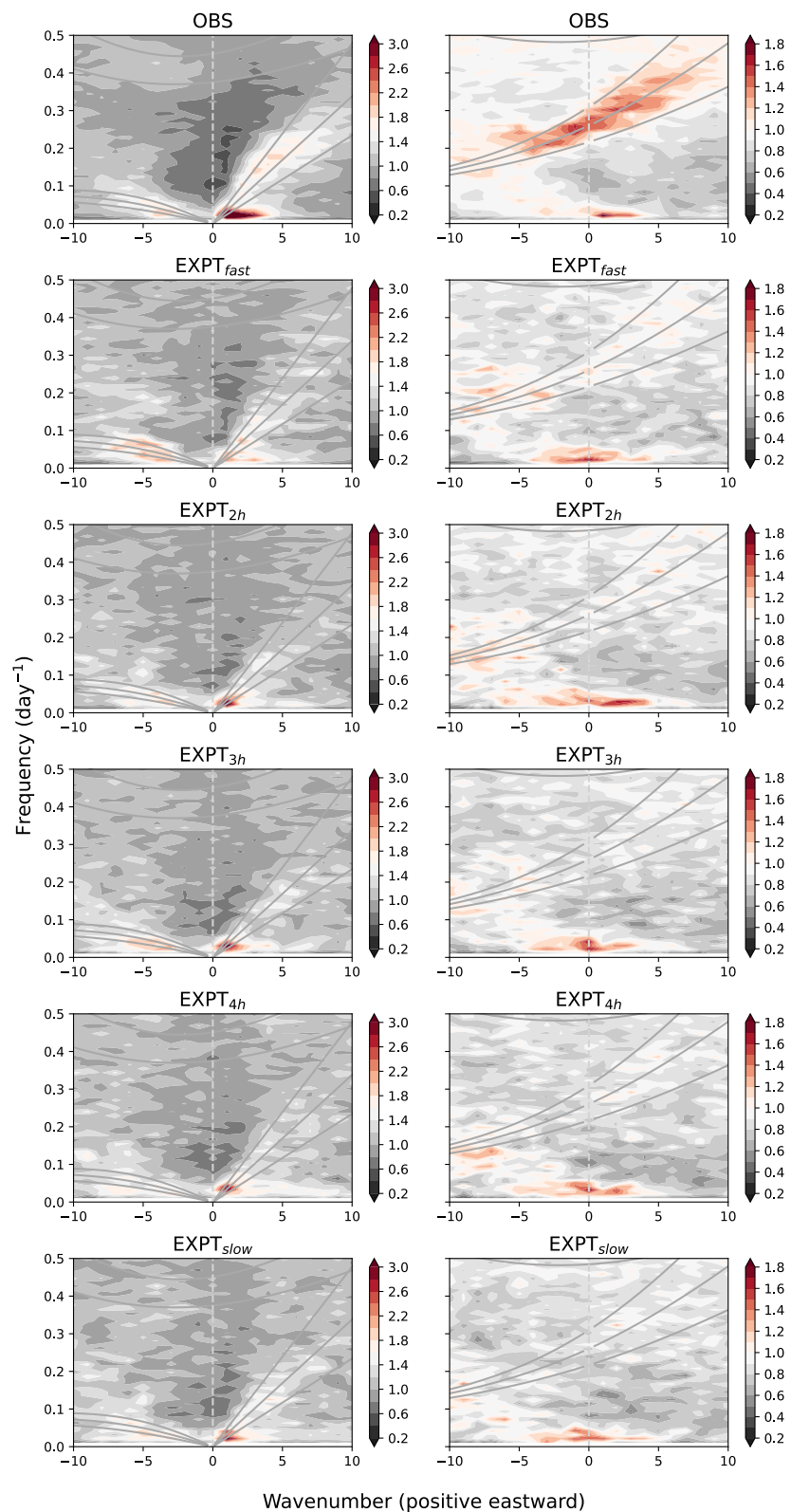


Figure 5. Takayabu-Wheeler-Kiladis spectra of outgoing long-wave radiation for OBS (from National Oceanic and Atmospheric Administration) and different experiments (as named above each panel), for the symmetric component (left-hand side panels) and antisymmetric component (right-hand side panels).

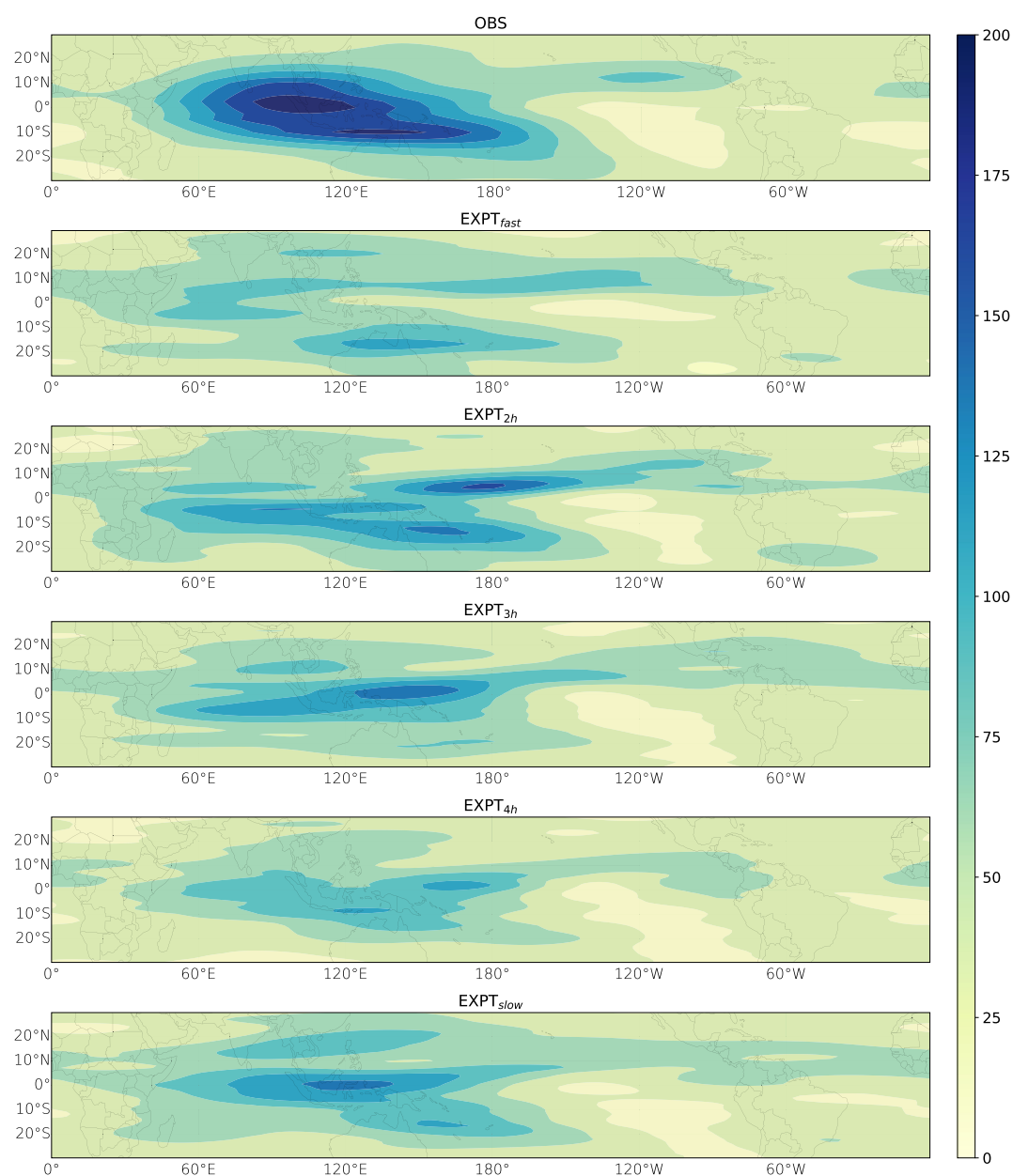


Figure 6. Madden–Julian oscillation variance computed as the daily variance of outgoing long-wave radiation data filtered for 1–5 wavenumber and 20–100 days frequency, for OBS (from National Oceanic and Atmospheric Administration) and different experiments (as named above each panel).

Each frame in Figure 7 depicts 10°S–10°N averaged cross-correlations of OLR anomalies with MJO-index. The MJO-index is defined as the 20–100-day filtered OLR anomalies averaged over 5°S–5°N, 75–85°E following Guo et al. (2015). It is noteworthy to mention, reiterating Guo et al. (2015), the philosophy behind using such an MJO index. An index based on a 20–100 days filter brings out the dominant intraseasonal signal in the data that ideally should be an MJO signal. The eastward propagating red and blue patches of correlation values in observations (Figure 7a) confirm it. We note the phase speed is faster over the west Pacific (east of ~120°E) than that over the Indian Ocean (west of ~100°E). The relatively slow phase speed in the longitude range ~100°–120°E is collocated with the Indonesian archipelago. These different phase speeds over land and oceanic regions are consistent with MJO interaction with the profound diurnal variations of meteorology over the MC. It furthermore emphasizes the need to mimic land-ocean heterogeneity realistically in climate models.

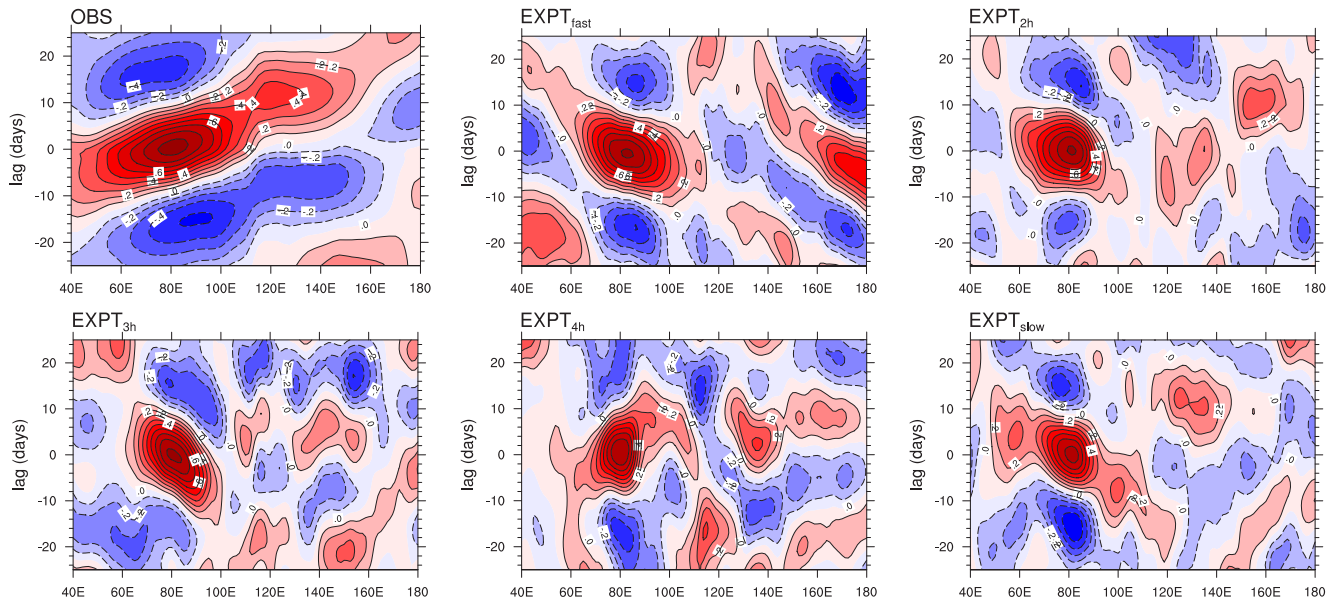


Figure 7. Madden–Julian oscillation propagation: Hovmöller (averaged from 10°S to 10°N) plots of cross-correlations of MJO-filtered outgoing long-wave radiation (OLR) (W m^{-2}) anomalies (Winter) with MJO-index (defined as the 20–100-day filtered OLR anomalies averaged over 5°S–5°N, 75–85°E), for OBS (from National Oceanic and Atmospheric Administration) and different experiments (as named above each panel).

To assess the performance of our different experiments in simulating MJO propagation features, we recall the “good” and “bad” models of Guo et al. (2015). In Figure 2, Guo et al. (2015) showed that the “good” models simulated more realistic eastward propagation than the “bad” models. In Figure 7, *EXPT_{4h}* is the only experiment with an eastward propagation and exhibits some resemblance with observations and the only “good” model, albeit with some key caveats. The positive anomalies almost abruptly died over the MC and reappeared over the western Pacific. Nonetheless, an intriguing observation, that contains the novelty of our research, is the more realistic eastward propagation simulated in *EXPT_{4h}* than in *EXPT_{slow}*. An improved simulation of eastward propagation in *EXPT_{4h}* supports our argument that using two τ for land and ocean is a logical choice. It reconfirms our anticipation that representing land–ocean heterogeneity via τ in ZM in CAM alters convective memory and affects the organization of convection. A larger τ_O than τ_L , although reasonable, is only based on intuition. A detailed sensitivity analysis would be required to investigate and underpin the best pair of τ values. It might involve exploring model sensitivity to the threshold value of CAPE for triggering deep convection (represented by the variable *capelmt* in the CAM code).

4. Discussion and Conclusion

4.1. Findings

Climate models continue to grow, fueled by a growing understanding of the earth system. Hence, it is only logical to include a fairly well-recognized and relatively old knowledge about land and ocean heterogeneity of atmospheric convection in the parameterization of convection. We argue that using two different τ in ZM in CAM can be one simple yet fruit-bearing way. In our experiments to investigate the model response to land–ocean heterogeneity in τ values, we used $\tau_L = 1$ hr, and $\tau_O = 2, 3, 4$ hr. In two additional experiments, *EXPT_{fast}* and *EXPT_{slow}*, we used $\tau_L = \tau_O = 1$ hr and $\tau_L = \tau_O = 4$ hr, respectively, to complement the previous group of experiments. The τ values that we have used are informed by our knowledge of frequency, life-cycle, and behavior of atmospheric convection over land and ocean learned from previous studies (Lucas et al., 1994; Williams & Stanfill, 2002; Zipser et al., 2006; Hagos et al., 2013; Matsui et al., 2016; Roca et al., 2017; Roca & Fiolleau, 2020) and inspired by results of relevant model sensitivity experiments (Lee et al., 2009; Mishra & Srinivasan, 2010; Mishra, 2011; Misra et al., 2012; Zhang & McFarlane, 1995).

Our findings regarding the model simulated mean state in different experiments are consistent with earlier studies (Lee et al., 2009; Mishra & Srinivasan, 2010; Mishra, 2011; Misra et al., 2012). For example, total rainfall

remained approximately the same while large-scale rainfall increased and convective rain decreased for longer τ_L s. Consistency of the model response for a slow τ only over the oceans with slowing down τ globally is most likely a result of 75% of the global surface being ocean. However, since there is no physical barrier between the atmospheric columns over continents and oceans, having two τ values in our experiments, which essentially are prescribed to represent heterogeneity in the persistence of convection over the two different surfaces, created a distinction between the intensities with which the model responses are felt over land and ocean. For example, the oceanic boundary layer is moister and warmer than the continental boundary layer (Figure S4b in Supporting Information S1). Furthermore, the mid-troposphere is drier and cooler over oceans than over the continents (Figure 2). These land-ocean heterogeneities inevitably create differences in atmospheric instabilities. These instabilities are essentially realized in the form of atmospheric convection that, by design in our experiments with slower τ , takes longer to bring the atmosphere back to a background state. It is suggestive of a longer persistence of convective instability over the ocean than that over the continents which essentially can be linked with memory of convection (Davies et al., 2009; Colin et al., 2019; Hwong et al., 2023).

The conclusion that the model simulated better MJO propagation characteristics in $EXPT_{4h}$ than in $EXPT_{slow}$ is a key. Scientists had advocated in favor of a slower τ in earlier studies (Donner & Phillips, 2003; Lee et al., 2009; Mishra, 2011; Misra et al., 2012; Zhao et al., 2018). We also note a significant increase in MJO power for $\tau = 4$ hr than $\tau = 1$ hr (comparing Figures 5b and 5f). However, an evaluation of the model simulated intraseasonal zonal propagation reveals that $EXPT_{4h}$ performs considerably better than $EXPT_{slow}$. This confirms that having one τ globally is not only unphysical but also slowing it down tinkering persistence of convection to improve simulation of equatorial waves may result in model responses that might look improved, but only superficially.

4.2. Long τ_L and Short τ_O

We performed a last experiment to evaluate the model sensitivity to τ . In this experiment, we prescribed $\tau_L = 4$ hr and $\tau_O = 1$ hr. The τ values in it are exactly inverse of $EXPT_{4h}$. We named this experiment $EXPT_{4hLand}$. The mean state in this experiment is almost similar as $EXPT_{4h}$ (and $EXPT_{slow}$). However, it simulates an unrealistic westward MJO propagation characteristics. Results from this simulation are provided in Supplementary section, ‘ $EXPT_{4hLand}$ results’. This last experiment $EXPT_{4hLand}$ emphasizes 3 key points that help us integrate earlier studies with ours and also provides valuable new insights about the model behavior.

- The $EXPT_{4h}$ and $EXPT_{4hLand}$ behave similarly as $EXPT_{slow}$ in Figures S8 and S9 in Supporting Information S1. This suggests that the model mean state is immune to land-ocean heterogeneity of τ and sensitive only to the slowest value of τ whether over ocean, land, or globally.
- Longer τ is preferable (consistent with earlier studies). Although the model mean state does not exhibit dramatic changes (panels a, b, and c, in Figures S8 and S9 in Supporting Information S1), the shape of the convective to total rainfall ratio is considerably more realistic for a longer τ , particularly the meridional profile over the ocean (orange, red, or dark blue curves in Figure S8f in Supporting Information S1), albeit with weak magnitude. The fact that $EXPT_{4hLand}$ exhibits a similar rainfall partitioning ratio as $EXPT_{4h}$ is intriguing and deserves further investigation. We speculate that the introduction of a convective memory by delaying the CAPE relaxation time scale is immune to geographical location despite being arguably unphysical. An unrealistic MJO propagation is a likely manifestation of it (discussed in the third bullet below).
- While the mean state of the model advocates for a longer τ , the need for land-ocean heterogeneity in τ emerges when we analyze the simulation of MJO in our experiments. In particular, the evaluation of the MJO propagation underpins a primary nature of the design of the heterogeneity, which is $\tau_O > \tau_L$ (as we conclude from Fig S12 in Supporting Information S1). Figures S10–S12 in Supporting Information S1 are extensions of Figures 5–7 and include results from $EXPT_{4hLand}$. The MJO propagation depicted in Figure S12 in Supporting Information S1 suggests that $EXPT_{4h}$ is the only experiment that simulates a hint of eastward propagation, and $EXPT_{4hLand}$ continues to simulate unrealistic MJO propagation, although not as unrealistic as $EXPT_{fast}$. To improve MJO (hence, possibly equatorial waves) simulation, two τ values are preferred with $\tau_O > \tau_L$.

Although the purpose of our results is to serve as a proof of concept, $EXPT_{4h}$ in Figures 3, 4 and 7 is already remarkable. The uncertainty of the best version of the model between $EXPT_{2h}$ (arguably the best model to simulate the mean climate) and $EXPT_{4h}$ (arguably the best model to simulate the MJO) raises a chronic issue of climate models' conflict of improving mean and the variability (Lin et al., 2006; Kim et al., 2011). A

comprehensive evaluation of the model mean state and equatorial wave's dynamical, thermodynamical, and structural characteristics in a fully coupled CAM model with two τ values remains as our top future research priority.

4.3. Model Response in the Midlatitudes

Convective parameterization development efforts are often guided by the physics and statistics of tropical clouds. Model responses in the middle latitudes are seldom evaluated or reported. Unfortunately, our study is also not free from this conventional approach. Nonetheless, we plotted the vertical cross-section of zonal mean climatological zonal winds. We have provided this figure in the supplementary document as Figure S13 in Supporting Information S1. Consistent with our analysis of the model mean state (Section 3.2), we note a reduction of bias in $EXPT_{2h}$ simulated zonal winds in the northern hemisphere middle-latitudes. From $EXPT_{fast}$ to $EXPT_{slow}$, in all the simulations, the zonal winds in the southern hemisphere remain almost immune to our experiments. It can be associated with much lesser land-ocean heterogeneity in the southern hemisphere compared to the northern hemisphere. Detailed analysis of model response in the middle latitudes would provide more insight. Improved simulation in the northern hemisphere is a promising aspect of our prescribed experimental τ values.

4.4. Recommendation and Limitations

Our results, in general, serve as proof of concept that a realistic representation of convective adjustment time scale over land and ocean is a logical requirement that properly implemented shall lead to improvements in climate model simulations. In specific, we advocate at least two τ values, one for the continents and one relatively slower for the oceans in ZM in CAM. The fact that we did not perform a rigorous model sensitivity analysis (e.g., Qian et al., 2015; Lin et al., 2016; Goswami et al., 2017) nor did we perform any cloud-resolving simulation targeting the life-cycle of atmospheric convection (Davies et al., 2013; Colin et al., 2019; Daleu et al., 2020, e.g.,) leaves a scope as well as the requirement for future research to determine the best values of τ_L and τ_O for ZM in CAM. It will hopefully guide convection parameterization schemes, especially the adjustment types, to address land-ocean heterogeneity. Specifically, we recommend that future developments of CAM should consider prescribing different τ_L and τ_O in ZM in CAM. While simply lengthening τ could result in better partitioning of rainfall into convective and stratiform, it might not be enough for simulating realistic equatorial waves.

A framework to mimic finer geographical variations of τ (Ahmed & Schumacher, 2017) would be an immediate next step (for example, Wang et al., 2024), with a goal set to a more fundamental framework to incorporate the detailed boundary layer processes realistically initiating deep convection (Donner & Phillips, 2003). It will help eliminate sensitive unbounded tunable parameters like τ . Until then, experiments like the ones documented in this study will remain critical in understanding these tunable parameters and prescribe realistic values, which hopefully shall help evaluate other aspects of model simulations with more confidence.

Data Availability Statement

- Model: We used the atmospheric model of the Community Earth System Model, version 2.1.3 (CESM 2.1.3) (Danabasoglu et al., 2020).
- Description of the model simulations is provided in Section 2 of the manuscript. A source file of CESM 2.1.3, zm_conv.F90, modified for our experiments is publicly available at Goswami et al. (2025).
- Data analysis software: Figures 1–6 were generated using Python, and Figure 7 was generated using NCL. The corresponding scripts are publicly available at Goswami et al. (2025).
- Model Output Data: The model simulation data used to produce Figures 1–7 are publicly available in Goswami et al. (2025).

References

- Ahmed, F., Adames, A. F., & Neelin, J. D. (2020). Deep convective adjustment of temperature and moisture. *Journal of the Atmospheric Sciences*, 77(6), 2163–2186. <https://doi.org/10.1175/JAS-D-19-0227.1>
- Ahmed, F., & Schumacher, C. (2017). Geographical differences in the tropical precipitation-moisture relationship and rain intensity onset. *Geophysical Research Letters*, 44(2), 1114–1122. <https://doi.org/10.1002/2016GL071980>
- Alapathy, K., Madala, R. V., & Raman, S. (1994). Numerical simulation of orographic-convective rainfall with Kuo and betts-miller cumulus parameterization schemes. *Journal of the Meteorological Society of Japan. Ser. II*, 72(1), 123–137. https://doi.org/10.2151/jmsj1965.72.1_123
- Alapathy, K., Raman, S., Madala, R. V., & Mohanty, U. C. (1994). Monsoon rainfall simulations with the Kuo and Betts-Miller schemes. *Meteorology and Atmospheric Physics*, 53(1–2), 33–49. <https://doi.org/10.1007/BF01031903>

Acknowledgments

The authors gratefully acknowledge funding from the European Research Council (ERC) under the European Union's Horizon 2020 research and innovation program (Project CLUSTER, Grant 805041). This research was supported by the Scientific Service Units (SSU) of ISTA through resources provided by Scientific Computing (SciComp). We would like to thank Prof. Courtney Schumacher and Dr. Aaron Funk of Texas A&M University for their help in understanding the TRMM Radar data. The authors are grateful to two anonymous reviewers who helped improve the quality of this paper.

- Arakawa, A. (2004). The cumulus parameterization problem: Past, present, and future. *Journal of Climate*, 17(13), 2493–2525. [https://doi.org/10.1175/1520-0442\(2004\)017<2493:RATCPP>2.0.CO;2](https://doi.org/10.1175/1520-0442(2004)017<2493:RATCPP>2.0.CO;2)
- Bechtold, P., Bazile, E., Guichard, F., Mascart, P., & Richard, E. (2001). A mass flux convection scheme for regional and global models. *Quarterly Journal of the Royal Meteorological Society*, 127(573), 869–886. <https://doi.org/10.1002/qj.49712757309>
- Bechtold, P., Köhler, M., Jung, T., Doblas-Reyes, F., Leutbecher, M., Rodwell, M. J., et al. (2008). Advances in simulating atmospheric variability with the ECMWF model: From synoptic to decadal time scales. *Quarterly Journal of the Royal Meteorological Society*, 134(634), 1337–1351. <https://doi.org/10.1002/qj.289>
- Betts, A. K. (1986). A new convective adjustment scheme. Part I: Observational and theoretical basis. *Quarterly Journal of the Royal Meteorological Society*, 112(473), 677–691. <https://doi.org/10.1002/qj.49711247307>
- Betts, A. K., & Miller, M. J. (1986). A new convective adjustment scheme. Part II: Single column tests using GATE wave, BOMEX, ATEX and arctic air mass data sets. *Quarterly Journal of the Royal Meteorological Society*, 112(473), 693–709. <https://doi.org/10.1002/qj.49711247308>
- Betts, A. K., & Miller, M. J. (1993). The betts-miller scheme. In *The representation of cumulus convection in numerical models* (pp. 107–121). American Meteorological Society. https://doi.org/10.1007/978-1-935704-13-3_9
- Bogenschutz, P. A., Gettelman, A., Hannay, C., Larson, V. E., Neale, R. B., Craig, C., & Chen, C.-C. (2018). The path to CAM6: Coupled simulations with CAM5.4 and CAM5.5. *Geoscientific Model Development*, 11(1), 235–255. <https://doi.org/10.5194/gmd-11-235-2018>
- Bretherton, C. S., Peters, M. E., & Back, L. E. (2004). Relationships between water vapor path and precipitation over the tropical oceans. *Journal of Climate*, 17(7), 1517–1528. [https://doi.org/10.1175/1520-0442\(2004\)017<1517:RBWVPA>2.0.CO;2](https://doi.org/10.1175/1520-0442(2004)017<1517:RBWVPA>2.0.CO;2)
- Bullock, O. R., Alapaty, K., Herwehe, J. A., & Kain, J. S. (2015). A dynamically computed convective time scale for the Kain-Fritsch convective parameterization scheme. *Monthly Weather Review*, 143(6), 2105–2120. <https://doi.org/10.1175/MWR-D-14-00251.1>
- Chen, D., Dai, A., & Hall, A. (2021). The Convective Total precipitation ratio and the Drizzling Bias in climate models. *Journal of Geophysical Research: Atmospheres*, 126(16), e2020JD034198. <https://doi.org/10.1029/2020JD034198>
- Colin, M., Sherwood, S., Geoffroy, O., Bony, S., & Fuchs, D. (2019). Identifying the sources of convective memory in cloud-resolving simulations. *Journal of the Atmospheric Sciences*, 76(3), 947–962. <https://doi.org/10.1175/JAS-D-18-0036.1>
- Dai, A. (2006). Precipitation characteristics in eighteen coupled climate models. *Journal of Climate*, 19(18), 4605–4630. <https://doi.org/10.1175/JCLI3884.1>
- Daleu, C. L., Plant, R. S., Woolnough, S. J., Stirling, A. J., & Harvey, N. J. (2020). Memory properties in Cloud-Resolving simulations of the diurnal cycle of deep convection. *Journal of Advances in Modeling Earth Systems*, 12(8), e2019MS001897. <https://doi.org/10.1029/2019MS001897>
- Danabasoglu, G., Lamarque, J., Bacmeister, J., Bailey, D. A., DuVivier, A. K., Edwards, J., et al. (2020). The community earth system model version 2 (CESM2). *Journal of Advances in Modeling Earth Systems*, 12(2), e2019MS001916. <https://doi.org/10.1029/2019MS001916>
- Davies, L. (2008). *Self-organisation of convection as a mechanism for memory*. Ph.D. thesis. The University of Reading.
- Davies, L., Plant, R. S., & Derbyshire, S. H. (2009). A simple model of convection with memory. *Journal of Geophysical Research*, 114(D17), 17202. <https://doi.org/10.1029/2008JD011653>
- Davies, L., Plant, R. S., & Derbyshire, S. H. (2013). Departures from convective equilibrium with a rapidly varying surface forcing. *Quarterly Journal of the Royal Meteorological Society*, 139(676), 1731–1746. <https://doi.org/10.1002/qj.2065>
- Donner, L. J., & Phillips, V. T. (2003). Boundary layer control on convective available potential energy: Implications for cumulus parameterization. *Journal of Geophysical Research*, 108(D22), 4701. <https://doi.org/10.1029/2003JD003773>
- Emanuel, K. A., David Neelin, J., & Bretherton, C. S. (1994). On large-scale circulations in convecting atmospheres. *Quarterly Journal of the Royal Meteorological Society*, 120(519), 1111–1143. <https://doi.org/10.1002/qj.49712051902>
- Fritsch, J. M., & Chappell, C. F. (1980). Numerical prediction of convectively driven mesoscale pressure systems. Part I: Convective parameterization. *Journal of the Atmospheric Sciences*, 37(8), 1722–1733. [https://doi.org/10.1175/1520-0469\(1980\)037<1722:NPOCDM>2.0.CO;2](https://doi.org/10.1175/1520-0469(1980)037<1722:NPOCDM>2.0.CO;2)
- Goswami, B. B., Khouider, B., Phani, R., Mukhopadhyay, P., & Majda, A. J. (2017). Implementation and calibration of a stochastic multicloud convective parameterization in the NCEP Climate Forecast System (CFSv2). *Journal of Advances in Modeling Earth Systems*, 9(3), 1721–1739. <https://doi.org/10.1002/2017MS001014>
- Goswami, B. B., Deshpande, M., Mukhopadhyay, P., Saha, S. K., Rao, S. A., Murthugudde, R., & Goswami, B. N. (2014). Simulation of monsoon intraseasonal variability in NCEP CFSv2 and its role on systematic bias. *Climate Dynamics*, 43(9–10), 2725–2745. <https://doi.org/10.1007/s00382-014-2089-5>
- Goswami, B. B., Krishna, R. P. M., Mukhopadhyay, P., Khairoutdinov, M., & Goswami, B. N. (2015). Simulation of the Indian summer monsoon in the superparameterized climate forecast system version 2: Preliminary results. *Journal of Climate*, 28(22), 8988–9012. <https://doi.org/10.1175/JCLI-D-14-00607.1>
- Goswami, B. B., Polesello, A., & Muller, C. (2025). CESM-2.1.3 model simulated data and analysis scripts for “An assessment of representing land-ocean heterogeneity via CAPE relaxation timescale in the Community Atmospheric Model 6 (CAM6)” [Dataset]. *Zenodo*. <https://doi.org/10.5281/zenodo.10911960>
- Grell, G. A., & Freitas, S. R. (2014). A scale and aerosol aware stochastic convective parameterization for weather and air quality modeling. *Atmospheric Chemistry and Physics*, 14(10), 5233–5250. <https://doi.org/10.5194/acp-14-5233-2014>
- Guo, Y., Waliser, D. E., & Jiang, X. (2015). A systematic relationship between the representations of convectively coupled equatorial wave activity and the Madden-Julian oscillation in climate model simulations. *Journal of Climate*, 28(5), 1881–1904. <https://doi.org/10.1175/JCLI-D-14-00485.1>
- Hagos, S., Feng, Z., McFarlane, S., & Leung, L. R. (2013). Environment and the lifetime of tropical deep convection in a cloud-permitting regional model simulation. *Journal of the Atmospheric Sciences*, 70(8), 2409–2425. <https://doi.org/10.1175/JAS-D-12-0260.1>
- Hersbach, H., Bell, B., Berrisford, P., Biavati, G., Horányi, A., Muñoz Sabater, J., et al. (2023). ERA5 monthly averaged data on pressure levels from 1940 to present. Copernicus Climate Change Service (C3S) Climate Data Store (CDS). *Tech. rep.* <https://doi.org/10.24381/cds.6860a573>
- Hourdin, F., Mauritsen, T., Gettelman, A., Golaz, J. C., Balaji, V., Duan, Q., et al. (2017). The art and science of climate model tuning. *Bulletin of the American Meteorological Society*, 98(3), 589–602. <https://doi.org/10.1175/BAMS-D-15-00135.1>
- Huffman, G. J., Bolvin, D. T., Nelkin, E. J., Wolff, D. B., Adler, R. F., Gu, G., et al. (2007). The TRMM multisatellite precipitation analysis (TMPA): Quasi-global, multiyear, combined-sensor precipitation estimates at fine scales. *Journal of Hydrometeorology*, 8(1), 38–55. <https://doi.org/10.1175/JHM560.1>
- Hwong, Y.-L., Colin, M., Aglas-Leitner, P., Muller, C., & Sherwood, S. (2023). *Assessing memory in convection schemes using idealized tests*. ESS Open Archive.
- Kain, J. S., & Fritsch, J. M. (1993). Convective parameterization for mesoscale models: The Kain-Fritsch scheme. In *The representation of cumulus convection in numerical models* (pp. 165–170). American Meteorological Society. https://doi.org/10.1007/978-1-935704-13-3_16

- Kalnay, E., Kanamitsu, M., Kistler, R., Collins, W., Deaven, D., Gandin, L., et al. (1996). The NCEP/NCAR 40-year reanalysis project. *Bulletin of the American Meteorological Society*, 77(3), 437–471. <https://www.taylorfrancis.com/chapters/edit/10.4324/9781315793245-16/ncep-ncar-40-year-reanalysis-project-kalnay-kanamitsu-kistler-collins-deaven-gandin-iredell-saha-white-woollen-zhu-chelliah-ebisuzaki-higgins-janowiak-mo-ropelewski-wang-leetmaa-reynolds-roy-jenne-dennis-joseph>
- Kim, D., Sobel, A. H., Maloney, E. D., Frierson, D. M. W., & Kang, I.-S. (2011). A systematic relationship between intraseasonal variability and mean state bias in AGCM simulations. *Journal of Climate*, 24(21), 5506–5520. <https://doi.org/10.1175/2011JCLI4177.1>
- Klotzbach, P. J. (2014). The Madden-Julian Oscillation's impacts on worldwide tropical cyclone activity. *Journal of Climate*, 27(6), 2317–2330. <https://doi.org/10.1175/JCLI-D-13-00483.1>
- Kumar, R., Pathak, R., Sahany, S., & Mishra, S. K. (2023). Indian summer monsoon simulations in successive generations of the NCAR Community Atmosphere Model. *Theoretical and Applied Climatology*, 153(3–4), 977–992. <https://doi.org/10.1007/s00704-023-04514-0>
- Kyselý, J., Rulfová, Z., Farda, A., & Hanel, M. (2016). Convective and stratiform precipitation characteristics in an ensemble of regional climate model simulations. *Climate Dynamics*, 46(1–2), 227–243. <https://doi.org/10.1007/s00382-015-2580-7>
- Lee, J. E., Pierrehumbert, R., Swann, A., & Lintner, B. R. (2009). Sensitivity of stable water isotopic values to convective parameterization schemes. *Geophysical Research Letters*, 36(23), L23801. <https://doi.org/10.1029/2009GL040880>
- Liebmman, B., & Smith, C. (1996). Description of a complete (interpolated) outgoing longwave radiation dataset. *Bulletin of the American Meteorological Society*, 77, 1275–1277.
- Lin, G., Wan, H., Zhang, K., Qian, Y., & Ghan, S. J. (2016). Can nudging be used to quantify model sensitivities in precipitation and cloud forcing? *Journal of Advances in Modeling Earth Systems*, 8(3), 1073–1091. <https://doi.org/10.1002/2016MS000659>
- Lin, J.-L., Kiladis, G. N., Mapes, B. E., Weickmann, K. M., Sperber, K. R., Lin, W., et al. (2006). Tropical intraseasonal variability in 14 IPCC AR4 climate models. Part I: Convective signals. *Journal of Climate*, 19(12), 2665–2690. <https://doi.org/10.1175/JCLI3735.1>
- Lin, X., Randall, D. A., & Fowler, L. D. (2000). Diurnal variability of the hydrologic cycle and radiative fluxes: Comparisons between observations and a GCM. *Journal of Climate*, 13(23), 4159–4179. [https://doi.org/10.1175/1520-0442\(2000\)013<4159:DVOTHC>2.0.CO;2](https://doi.org/10.1175/1520-0442(2000)013<4159:DVOTHC>2.0.CO;2)
- Lucas, C., Zipser, E. J., & Lemone, M. A. (1994). Vertical velocity in oceanic convection off tropical Australia. *Journal of the Atmospheric Sciences*, 51(21), 3183–3193. [https://doi.org/10.1175/1520-0469\(1994\)051<3183:VVIICO>2.0.CO;2](https://doi.org/10.1175/1520-0469(1994)051<3183:VVIICO>2.0.CO;2)
- Maloney, E. D., & Hartmann, D. L. (2000). Modulation of eastern North Pacific hurricanes by the Madden-Julian oscillation. *Journal of Climate*, 13(9), 1451–1460. [https://doi.org/10.1175/1520-0442\(2000\)013<1451:MOENPH>2.0.CO;2](https://doi.org/10.1175/1520-0442(2000)013<1451:MOENPH>2.0.CO;2)
- Maloney, E. D., & Hartmann, D. L. (2000). Modulation of hurricane activity in the Gulf of Mexico by the Madden-Julian oscillation. *Science*, 287(5460), 2002–2004. <https://doi.org/10.1126/science.287.5460.2002>
- Maloney, E. D., & Kiehl, J. T. (2002). MJO-related SST variations over the tropical eastern Pacific during northern hemisphere summer. *Journal of Climate*, 15(6), 675–689. [https://doi.org/10.1175/1520-0442\(2002\)015<0675:MRSVOT>2.0.CO;2](https://doi.org/10.1175/1520-0442(2002)015<0675:MRSVOT>2.0.CO;2)
- Matsui, T., Chern, J. D., Tao, W. K., Lang, S., Satoh, M., Hashino, T., & Kubota, T. (2016). On the land-ocean contrast of tropical convection and microphysics statistics derived from TRMM satellite signals and global storm-resolving models. *Journal of Hydrometeorology*, 17(5), 1425–1445. <https://doi.org/10.1175/JHM-D-15-0111.1>
- Mayta, V. C., & Adames Corraliza, A. F. (2023). Is the madden-julian oscillation a moisture mode? *Geophysical Research Letters*, 50(15), e2023GL103002. <https://doi.org/10.1029/2023GL103002>
- Mishra, S. K. (2011). Influence of convective adjustment time scale on the tropical transient activity. *Meteorology and Atmospheric Physics*, 114(1), 17–34. <https://doi.org/10.1007/s00703-011-0154-8>
- Mishra, S. K. (2012). Effects of convective adjustment time scale on the simulation of tropical climate. *Theoretical and Applied Climatology*, 107(1–2), 211–228. <https://doi.org/10.1007/s00704-011-0479-8>
- Mishra, S. K., & Srinivasan, J. (2010). Sensitivity of the simulated precipitation to changes in convective relaxation time scale. *Annales Geophysicae*, 28(10), 1827–1846. <https://doi.org/10.5194/ANGE-28-1827-2010>
- Misra, V., Pantina, P., Chan, S., & DiNapoli, S. (2012). A comparative study of the Indian summer monsoon hydroclimate and its variations in three reanalyses. *Climate Dynamics*, 39(5), 1149–1168. <https://doi.org/10.1007/s00382-012-1319-y>
- Moorthi, S., & Suarez, M. J. (1992). Relaxed Arakawa-Schubert. A parameterization of moist convection for general circulation models. *Monthly Weather Review*, 120(6), 978–1002. [https://doi.org/10.1175/1520-0493\(1992\)120<0978:RASAP0>2.0.CO;2](https://doi.org/10.1175/1520-0493(1992)120<0978:RASAP0>2.0.CO;2)
- Pendergrass, A. G., & Hartmann, D. L. (2014). Changes in the distribution of rain frequency and intensity in response to global warming. *Journal of Climate*, 27(22), 8372–8383. <https://doi.org/10.1175/JCLI-D-14-00183.1>
- Qian, Y., Yan, H., Hou, Z., Johannesson, G., Klein, S., Lucas, D., et al. (2015). Parametric sensitivity analysis of precipitation at global and local scales in the Community Atmosphere Model CAM5. *Journal of Advances in Modeling Earth Systems*, 7(2), 382–411. <https://doi.org/10.1002/2014MS000354>
- Randall, D., Khairoutdinov, M., Arakawa, A., & Grabowski, W. (2003). Breaking the cloud parameterization deadlock. *Bulletin of the American Meteorological Society*, 84(11), 1547–1564. <https://doi.org/10.1175/BAMS-84-11-1547>
- Randall, D. A. (2013). Beyond deadlock. *Geophysical Research Letters*, 40(22), 5970–5976. <https://doi.org/10.1002/2013GL057998>
- Rayner, N. A., Parker, D. E., Horton, E. B., Folland, C. K., Alexander, L. V., Rowell, D. P., et al. (2003). Global analyses of sea surface temperature, sea ice, and night marine air temperature since the late nineteenth century. *Journal of Geophysical Research*, 108(D14), 4407. <https://doi.org/10.1029/2002JD002670>
- Rio, C., Del Genio, A. D., & Hourdin, F. (2019). Ongoing breakthroughs in convective parameterization. *Current Climate Change Reports* 2019, 5(2), 95–111. <https://doi.org/10.1007/s40641-019-00127-w>
- Roca, R., & Fiolleau, T. (2020). Extreme precipitation in the tropics is closely associated with long-lived convective systems. *Communications Earth and Environment*, 1(1), 1–6. <https://doi.org/10.1038/s43247-020-00015-4>
- Roca, R., Fiolleau, T., & Bouniol, D. (2017). A simple model of the life cycle of mesoscale convective systems cloud shield in the tropics. *Journal of Climate*, 30(11), 4283–4298. <https://doi.org/10.1175/JCLI-D-16-0556.1>
- Scinocca, J. F., & McFarlane, N. A. (2004). The variability of modeled tropical precipitation. *Journal of the Atmospheric Sciences*, 61(16), 1993–2015. [https://doi.org/10.1175/1520-0469\(2004\)061<1993:TVOMTP>2.0.CO;2](https://doi.org/10.1175/1520-0469(2004)061<1993:TVOMTP>2.0.CO;2)
- Shin, J., & Baik, J. (2023). Global simulation of the Madden-Julian oscillation with stochastic unified convection scheme. *Journal of Advances in Modeling Earth Systems*, 15(7), e2022MS003578. <https://doi.org/10.1029/2022MS003578>
- Stevens, B., Satoh, M., Auger, L., Biercamp, J., Bretherton, C. S., Chen, X., et al. (2019). DYAMOND: The DYNAMics of the atmospheric general circulation modeled on non-hydrostatic domains. *Progress in Earth and Planetary Science*, 6(1), 1–17. <https://doi.org/10.1186/s40645-019-0304-z>
- Sun, Y., Solomon, S., Dai, A., & Portmann, R. W. (2006). How often does it rain? *Journal of Climate*, 19(6), 916–934. <https://doi.org/10.1175/JCLI3672.1>

- Takayabu, Y. (1994). Large-scale cloud disturbances associated with equatorial waves. *Journal of the Meteorological Society of Japan. Ser. II*, 72(3), 433–449. https://doi.org/10.2151/jmsj1965.72.3_433
- Takayabu, Y. (1994). Large-scale cloud disturbances associated with equatorial waves. *Journal of the Meteorological Society of Japan. Ser. II*, 72(3), 451–465. https://doi.org/10.2151/jmsj1965.72.3_451
- Trmm, R. (2017). *README document for the tropical rainfall measurement mission (TRMM) version 7*, tech. Rep. Goddard Earth Sciences Data and Information Services Center (GES DISC).
- Wang, M., Wang, L., Wu, Q., & Cheng, H. (2024). Dynamically computed characteristic adjustment time scale for Zhang-McFarlane convective parameterization scheme. *Climate Dynamics*, 62(3), 2419–2437. <https://doi.org/10.1007/s00382-023-07031-y>
- Wheeler, M., & Kiladis, G. N. (1999). Convectively coupled equatorial waves: Analysis of clouds and temperature in the wavenumber-frequency domain. *Journal of the Atmospheric Sciences*, 56(3), 374–399. [10.1175/1520-0469\(1999\)056<0374:CCEWAO>2.0.CO;2](https://doi.org/10.1175/1520-0469(1999)056<0374:CCEWAO>2.0.CO;2)
- Williams, E., & Stanfill, S. (2002). The physical origin of the land-ocean contrast in lightning activity. *Comptes Rendus Physique*, 3(10), 1277–1292. [https://doi.org/10.1016/S1631-0705\(02\)01407-X](https://doi.org/10.1016/S1631-0705(02)01407-X)
- Woelfle, M. D., Bretherton, C. S., Hannay, C., & Neale, R. (2019). Evolution of the double-ITCZ bias through CESM2 development. *Journal of Advances in Modeling Earth Systems*, 11(7), 1873–1893. <https://doi.org/10.1029/2019MS001647>
- Yang, B., Qian, Y., Lin, G., Leung, L. R., Rasch, P. J., Zhang, G. J., et al. (2013). Uncertainty quantification and parameter tuning in the CAM5 Zhang-McFarlane convection scheme and impact of improved convection on the global circulation and climate. *Journal of Geophysical Research: Atmospheres*, 118(2), 395–415. <https://doi.org/10.1029/2012JD018213>
- Zhang, C., Adames, F., Khouider, B., Wang, B., & Yang, D. (2020). Four theories of the Madden-Julian oscillation. *Reviews of Geophysics*, 58(3), e2019RG000685. <https://doi.org/10.1029/2019RG000685>
- Zhang, G. J., & McFarlane, N. A. (1995). Sensitivity of climate simulations to the parameterization of cumulus convection in the Canadian climate centre general circulation model. *Atmosphere-Ocean*, 33(3), 407–446. <https://doi.org/10.1080/07055900.1995.9649539>
- Zhang, G. J., & Song, X. (2009). Interaction of deep and shallow convection is key to Madden-Julian Oscillation simulation. *Geophysical Research Letters*, 36(9), L09708. <https://doi.org/10.1029/2009GL037340>
- Zhao, M., Golaz, J., Held, I. M., Guo, H., Balaji, V., Benson, R., et al. (2018). The GFDL global atmosphere and land model AM4.0/LM4.0: 2. Model description, sensitivity studies, and tuning strategies. *Journal of Advances in Modeling Earth Systems*, 10(3), 735–769. <https://doi.org/10.1002/2017MS001209>
- Zhou, X., Atlas, R., McCoy, I. L., Bretherton, C. S., Bardeen, C., Gettelman, A., et al. (2021). Evaluation of cloud and precipitation simulations in CAM6 and AM4 using observations over the southern ocean. *Earth and Space Science*, 8(2), e2020EA001241. <https://doi.org/10.1029/2020EA001241>
- Zipser, E. J., Cecil, D. J., Liu, C., Nesbitt, S. W., & Yorty, D. P. (2006). Where are the most: Intense thunderstorms on Earth? *Bulletin of the American Meteorological Society*, 87(8), 1057–1071. <https://doi.org/10.1175/BAMS-87-8-1057>